

# Analysis of short and long range atomic order in nanocrystalline diamonds with application of powder diffractometry

B. Palosz<sup>\*,I</sup>, E. Grzanka<sup>I,II</sup>, S. Gierlotka<sup>I</sup>, S. Stel'makh<sup>I</sup>, R. Pielaszek<sup>I,II</sup>, U. Bismayer<sup>II</sup>, J. Neuefeind<sup>III</sup>, H.-P. Weber<sup>IV</sup>, Th. Proffen<sup>V</sup>, R. Von Dreele<sup>V</sup> and W. Palosz<sup>VI</sup>

<sup>I</sup> High Pressure Research Center UNIPRESS, Polish Academy of Sciences, ul. Sokolowska 29/37, PL-01 142 Warsaw, Poland

<sup>II</sup> Universität Hamburg, Mineralogisch-Petrographisches Institut, Grindelallee 48, D-20146 Hamburg, Germany

<sup>III</sup> HASYLAB at DESY, Notkestr. 85, D-22603 Hamburg, Germany

<sup>IV</sup> SNBL at ESRF, BP 220, Av des Martyrs, F-38043 Grenoble, France

<sup>V</sup> Los Alamos National Laboratory, LANSCE-12, Mailstop H805, Los Alamos, New Mexico, 87545, USA

<sup>VI</sup> USRA/NASA-Marshall Space Flight Center, SD46, Huntsville, Alabama 35812, USA

*Dedicated to Zeitschrift für Kristallographie on the occasion of its 125<sup>th</sup> anniversary<sup>1</sup>*

Received May 15, 2002; accepted August 6, 2002

**Abstract.** Fundamental limitations, with respect to nanocrystalline materials, of the traditional elaboration of powder diffraction data like the Rietveld method are discussed. A tentative method of the analysis of powder diffraction patterns of nanocrystals based on the examination of the variation of lattice parameters calculated from individual Bragg lines (named the “*apparent lattice parameter*”, *alp*) is introduced. We examine the application of our methodology using theoretical diffraction patterns computed for models of nanocrystals with a perfect crystal lattice and for grains with a two-phase, core-shell structure. We use the method for the analysis of X-ray and neutron experimental diffraction data of nanocrystalline diamond powders of 4, 6 and 12 nm in diameter. The effects of an internal pressure and strain at the grain surface are discussed. The results are based on the dependence of the *alp* values on the diffraction vector *Q* and on the PDF analysis. It is shown, that the experimental results lend a strong support to the concept of a two-phase structure of nanocrystalline diamond.

## 1. Introduction

In conventional polycrystalline materials with micrometer size grains the surface contains only an insignificant fraction of the total number of atoms and its effect on the overall properties of the material can be ignored. The situation is different in small, nano-size particles where, due to their size, a considerable fraction of the atoms forms the surface of the grain. An abrupt termination of a perfect crystal lattice leaves the outmost atoms without some of their neighbors which leads either to a reconstruction of

the surface or to generation of strains through changes in the lengths of interatomic bonds. In very small objects (a few nm in diameter) the number of surface-related atoms can exceed the number of the “bulk” atoms.

So far, in basic characterization of nanocrystalline powders reported in the literature, a presence of distinct surface layer is usually acknowledged but largely ignored [1–6]. The reason for this negligence is very simple: no information on the specific arrangement of atoms at the surface of nanograins is available and, so far, no experimental methods have been developed for the structural analysis of the surface of such small objects. This work presents an analysis of the applicability of powder diffraction techniques for elucidation of the atomic structure of nanocrystals, particularly that of the surface shell.

Although there is a general understanding that the surface has a significant effect on the physical properties of nanocrystals, the unique properties of these materials are being related to the size of the grains without regard to a specific atomic structure, particularly that of their surface. A number of literature reports on the dependence of different physical properties on the size of nanoparticles exist [7–15]. The observed changes of physical properties of materials in general, and crystals in particular are always related to changes of local and/or overall atomic arrangements and are usually accompanied by changes in the structure symmetry. While the specific atomic structures of nanocrystals have not been a subject of extended studies yet, different properties of the materials relative to those of the bulk crystals are often related to changes of their lattice parameters. A dependence of the lattice parameters on the grain size have been reported for a variety of nanomaterials, like metals (Au [16, 17], Al [18], Cu [19]), semiconductors (CdSe [20], GaN [21]), ionic crystals (NaCl, KCl, NaBr, LiF [22], Se [23], Y<sub>2</sub>O<sub>3</sub> [24]), and others. Those results are often attributed to the presence of a strong (homogeneous) “internal pressure” caused by the

\* Correspondence author (e-mail: PALOSZ@unipress.waw.pl)

<sup>1</sup> Due to the tight time schedule this contribution could not be published in the Celebration Issue No. 7–8 (2002).

surface stresses analogous to the surface tension in liquids [25–34]. This “straightforward” interpretation of the experimental findings ignores the fact, that the structure of a nanocrystal is not uniform and should be considered as composed of two distinctive, grain core and shell phases or (if this concept, for whatever reason, is not acceptable) one has to take into account at least the fact that a large fraction of the atoms at the grain surface is displaced relative to their regular lattice positions. In none of these cases should only one set of the lattice parameters be used for a unique characterization of the crystal.

Surface tension always develops at the surfaces separating different phases, bulk, liquid, or gaseous [26]. This phenomenon plays a significant role in determining the physico-chemical state of the system. The layer separating the phases is called an interface, interphase, or surface phase. In the literature it is common to refer to the model of surface tension introduced in 1805 by Young for a convenient description of all mechanical phenomena related to the presence of interphases, i.e. to situations where the system behaves as if consisting of two homogenous phases separated by a uniformly stretched membrane of infinitesimal thickness (representing the surface under tension). This is a rough simplification, which is quite satisfactory for a description of large volume materials but not adequate for an analysis of the atomic structure of interfaces.

In solids, the variation in the magnitude of the tension between the bulk and the surface can manifest itself macroscopically by a phenomenon analogous to the surface tension in liquids. In a uniform crystal lattice the chemical potential at the surface is greater than that in the bulk, therefore the surface atoms tend to diffuse towards the interior leaving vacancies at the surface. In a solid an exchange of particles between the surface and the bulk is very limited. The tendency for the atoms to diffuse in is demonstrated/realized through changes in the spacings, normal to the surface, between the last few layers of molecules, or through changes in the polarization state of the molecules. This is equivalent to a presence of strain in the vicinity of the surface, and may lead to an increase in the surface tension and to a reduction in its chemical potential. The strain may be expected to extend over several interatomic distances in the direction normal to the surface [35–38].

A nanocrystalline sample constitutes a polycrystalline material, thus the appropriate technique for determination of its atomic structure is powder diffraction. The present, well established standard of elaboration of powder diffraction data is based on the Rietveld method that is closely related to Bragg-type scattering [39, 40]. This method is also recommended and often used for structural analysis of nanocrystals. It is somehow overlooked by many researchers that this methodology has been developed and is dedicated to examination of long-range atomic order. Nanocrystals show a long-range order that is, however, limited by the size of the grains and, therefore, application of methods that are derived for infinite lattices may be inadequate [41, 42]. In this paper we show, that routine methods of powder diffraction data elaboration may lead to erroneous interpretation of the experimental results. We show that the description of the crystallographic structure of such materials based on the unit cell concept is defi-

nately insufficient if based on one set of lattice parameters alone: an interpretation of powder diffraction data of nanocrystals based on one unique set of lattice parameters is not possible. Accordingly, application of the lattice parameters concept, which is well defined only for one-phase perfect crystalline materials, has to be used with a special care when applied to characterization of the structure of nanocrystals. Recently we discussed applicability of a conventional powder diffractometry to structural studies of nanocrystals and suggested a replacement of the lattice parameters, which describe the dimensions (and shape) of the unit cell, by a set of values of the lattice parameters, each associated with (determined from) an individual Bragg reflection [41]. In other words, we suggest to link each lattice parameter calculated from a given powder diffraction pattern with the related diffraction vector  $Q$ . In this paper we present the results of the application of our concept, the “*apparent lattice parameters*” (*alp*) methodology, to elaboration of powder diffraction data of nanodiamond and for verification of the core-shell concept of nanocrystals. We applied also a complementary, alternate elaboration of the experimental diffraction data, the PDF analysis, and obtained the Atomic Pair Distribution Functions ( $G(r)$ ) from neutron diffraction data. The results on long-range order obtained with the *alp* analysis were compared with those obtained for short-range order with the PDF method.

## 2. Powder diffraction

The analysis of a powder diffraction data is routinely performed using the Bragg equation and elaboration methods like that of the Rietveld program based on the concept of the unit cell [39, 40]. Although possible in principle, it is impossible in practice to derive information on the local atomic arrangements using the Rietveld or similar programs. An alternate method of elaboration of powder diffraction data, developed for materials showing a short range order (like liquids and glasses) is the PDF analysis leading to determination of the Atomic Pair Distribution Function,  $G(r)$  [43–46]. Although PDF method is dedicated to the analysis of short-range order, it can also provide information on long-range atomic order as well.

Nanocrystals, although very small are, by definition, single crystals. As such, they belong to the class of materials with a long-range atomic order. However, this classification is not that obvious and may even be ambiguous because, in nano-sized grains, the long-range order is limited by the size of the crystallite that can be smaller than the coherence length of the scattered beam. Moreover, any atoms at the surface, which do not contribute to the coherent scattering of the atoms in the grain volume, do not contribute to the Bragg-type but to diffuse scattering. In PDF analysis this problem does not exist, since all scattered intensities are analyzed and contribution from all atoms is accounted for [44].

Both methods of elaboration of powder diffraction data have their advantages and disadvantages. Some of them are particularly important for structural analysis of nanocrystals. As we discuss in the following sections, for very

small crystallites the Bragg-type scattering is very sensitive to the grain size and shape and, thus, can provide information on these parameters of the material. On the other hand, a strong influence of the grains size and shape on Bragg scattering makes the analysis of the atomic structure particularly difficult. PDF analysis is insensitive to the grain size and shape and, therefore, provides straightforward information on the interatomic distances in the structure. Another difference between Bragg and PDF methods is, that while the analysis of Bragg scattering can be performed using any range of the diffraction vector  $Q$ , the resolution of PDF is very strongly dependent on the analyzed  $Q$ -range and requires collecting the diffraction data in a large  $Q$ -range. That cannot be accomplished using standard laboratory radiation sources. In this work we present the results of examination of nanocrystalline diamond powders using both elaboration methods and synchrotron and neutron powder diffraction data.

### 3. Bragg approach: examination of long-range order in nanocrystals

The simplest information that can be derived from a diffraction pattern is the lattice parameters. They are determined routinely based on the Bragg equation that relates lattice parameters to the positions of the intensity maxima of the diffraction patterns. According to Bragg, if a unit cell represents a given structure, the locations of the intensity maxima are determined uniquely by the specific interplanar spacings  $d_{hkl}$ . Determination of several Bragg reflections is sufficient to determine the symmetry, shape, and dimensions of the unit cell. This approach requires that the fundamental underlying assumptions of a perfect lattice be met, i.e.,

- (i), *the unit cell of the lattice is identical throughout the entire volume of the sample*, and,
- (ii), *the lattice is an array of points in space in which the environment of each point is identical*.

These conditions are never strictly met but, for larger crystallites, the deviations from the ideal model are negligible. For nanocrystals with sizes within the range of several nanometers the number of atoms associated with the surface and having the coordination number different than those in the bulk is significant and assumption (ii) is definitely not fulfilled. Therefore, for fundamental reasons, the methods of the structural analysis developed for crystalline materials with unique structures cannot yield satisfactory results for nanocrystals.

#### 3.1 Elaboration of a perfect powder diffraction experiment: limits of applicability of the Bragg equation

Relatively small number of atoms forming a nanocrystal provides a unique opportunity to build complete, atom-by-atom, models of small crystals. For such models one can calculate directly the Atomic Pair Distribution Function  $G(r)$  and, using the Debye equations, get the corresponding diffraction patterns. For technical reasons, direct calculations of the diffraction effects can be achieved for rela-

tively small arrays of atoms only. A moderate CPU time, on the order of hours, is sufficient to complete one calculation of the diffraction pattern only for nanoparticles smaller than 20 nm in diameter [47, 48].

To verify the applicability of the Bragg approach to nanoparticles, we calculated theoretical diffraction patterns of crystallographically perfect diamond nanocrystals. In other words, we simulated a perfect diffraction experiment where, (i), the beam is strictly parallel, (ii), no instrumental line broadening is present, and, (iii), the diffraction vector is known with ultimate accuracy. Our virtual “perfect experiment” does not require any instrument- and sample-related corrections. In principle, to elaborate the data and obtain the lattice parameters with absolute accuracy it is sufficient to read the positions of the Bragg lines. To determine the positions we fitted the line shapes using the pseudo-Voigt function (PeakFit 4.0 for Windows from SPSS Science).

We calculated the Atomic Pair Distribution Functions for diamond nanocrystals with different shapes and sizes (Fig. 1) and then, using the Debye equations, we computed the corresponding diffraction patterns from which we determined the positions of the Bragg lines used to calculate the corresponding parameter  $a$  of the cubic diamond unit cell. In Fig. 2 the values of  $a$  calculated from the first (111) Bragg reflection for crystallites with different shapes (Fig. 1) and dimensions are plotted versus the grain size. (In Fig. 2 the results for non-spherical crystallites are given at the Equivalent Sphere Diameter values,  $D_e$  which correspond to the diameter of a spherical crystal with the same number of atoms in the grain.) As seen in the graph, despite the fact that for all our models the same value of the lattice parameter ( $a_0 = 3.5668 \text{ \AA}$ ) was used, very large differences between the calculated lattice parameter values obtained for different models exist. Therefore, the calculated values of the “lattice parameter” are marked not as “ $a$ ” but “ $alp$ ” (the “apparent lattice parameter”, [41]). The deviation of the calculated  $alp$  values from the real value  $a_0$  increases both with a decrease of the number of atoms in the grain and with an

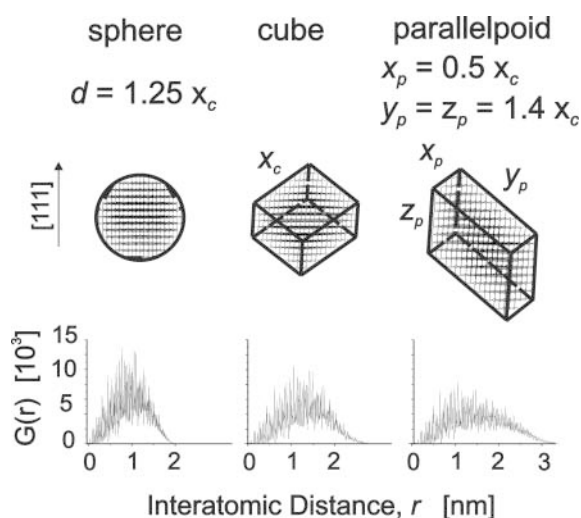


**Fig. 1.** Atomic Pair Distribution Function,  $G(r)$  (the number of atomic pairs, C–C, being at a distance  $r$ ) calculated for three different shapes of diamond nano-grains containing 1,500 atoms.

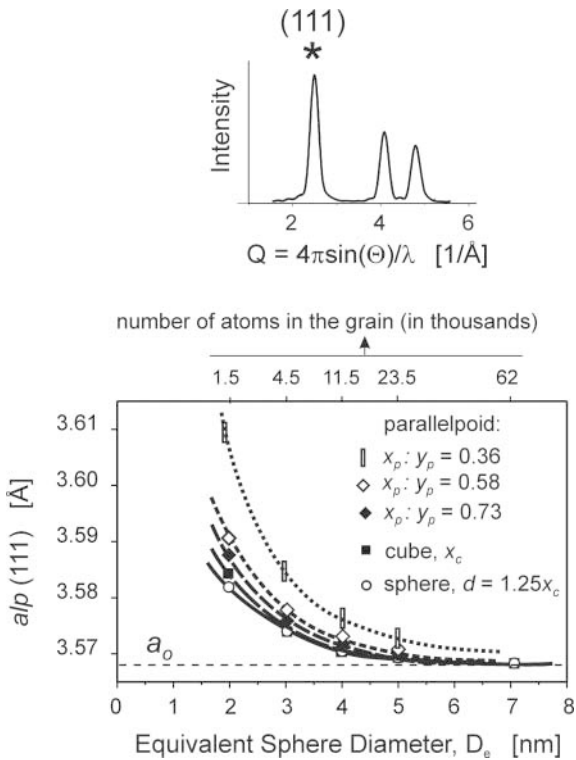


**Fig. 2.** Lattice parameter of cubic diamond as a function of the grain size determined from (111) Bragg reflection of theoretical diffraction patterns calculated for nanocrystals with different grain shapes shown in Fig. 1. Note that the calculated values of the lattice parameters are denoted as the *apparent lattice parameter*,  $alp$ .

increase in the shape anisotropy of the grains. As seen from the plot, a determination of the lattice parameters from a single reflection (111) is meaningless, unless the number of atoms in the grain is sufficiently large. According to Fig. 2, accurate value of  $a$  from a single reflection can be obtained if the grain is spherical and has the diameter larger than 8 nm; for anisotropic grains their size, in terms of the total volume, must be much larger.

Examination of the calculated patterns in a large diffraction vector range shows, that the position of not only (111) but of all Bragg-type reflections is affected by the grain size and shape. Fig. 3 shows  $alp$  values calculated from individual diffraction peaks of the theoretical patterns of grains with three different shapes. (For very broad maxima of the smallest grains, 2–3 nm, the accuracy of determination of the peak positions corresponds to uncertainty in  $alp$  of about 0.002 Å. For larger grains this uncertainty is 0.001 Å or less.) The individual  $alp$  values are plotted versus the diffraction vector  $Q$  of the Bragg reflections (We call them Bragg-like reflections, since they do not correspond to the real value of the unit cell parameters). As seen in the figure, for small crystals (at least up to the 8 nm grain examined in this work) no single Bragg-like reflection is in the position corresponding to that of the unit cell of the diamond lattice. The deviations of the  $alp$  values from the  $a_0$  parameter are smallest for spherical grains and increase with an increase in the anisotropy of the grain shape. In all cases the deviations of  $alp$  values calculated for individual Bragg-like reflections decrease with an increase in the diffraction vector  $Q$ . One should notice that in a routine powder diffraction experiment per-

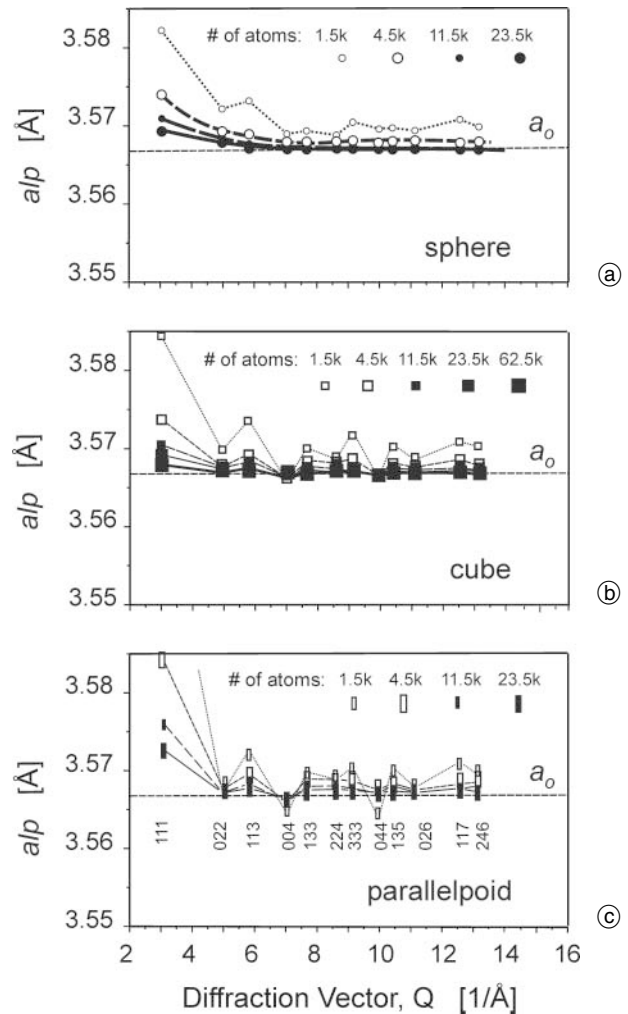


**Fig. 3.**  $Alp$ - $Q$  plots determined for individual Bragg reflections from the theoretical diffraction patterns of diamond with a perfect crystal lattice but different number of atoms in the grain, calculated for different grain shapes. (a), sphere; (b), cube; (c), parallelpiped.

formed using CuK or MoK radiation the available  $Q$ -range is only several  $\text{\AA}^{-1}$ . From our analysis it is obvious, that the lattice parameters calculated from such patterns for nanocrystalline materials with sizes smaller than 10 nm are unavoidably incorrect.

Determination of  $alp$  values for individual reflections that, for small crystallites, are broad and overlap is not always unambiguous and often impossible. Therefore, we suggest an alternate elaboration of powder diffraction patterns of nanocrystals based on refinement of the lattice parameters for selected ranges of the diffraction pattern, i.e. calculation of lattice parameters not for individual but for groups of reflections. Fig. 4 shows two kinds of  $alp$ - $Q$  plots obtained from theoretical diffraction patterns of a cube-shaped diamond nanocrystal containing 1,500 atoms. The top graph (Fig. 4a) shows the  $alp$  values calculated for individual reflections, the bottom one (Fig. 4b) shows the  $alp$  values obtained for selected groups of reflections (and drawn in the middle of a given  $Q$ -range). The dotted lines, connecting  $alp$  values of individual reflections (Fig. 4a), emphasize the non-monotonic relation of  $alp$  and the diffraction vector. The (averaged)  $alp$  values in Fig. 4b are the basis for the solid curve that emphasizes the general trend of  $alp$  with changing  $Q$  value. The same

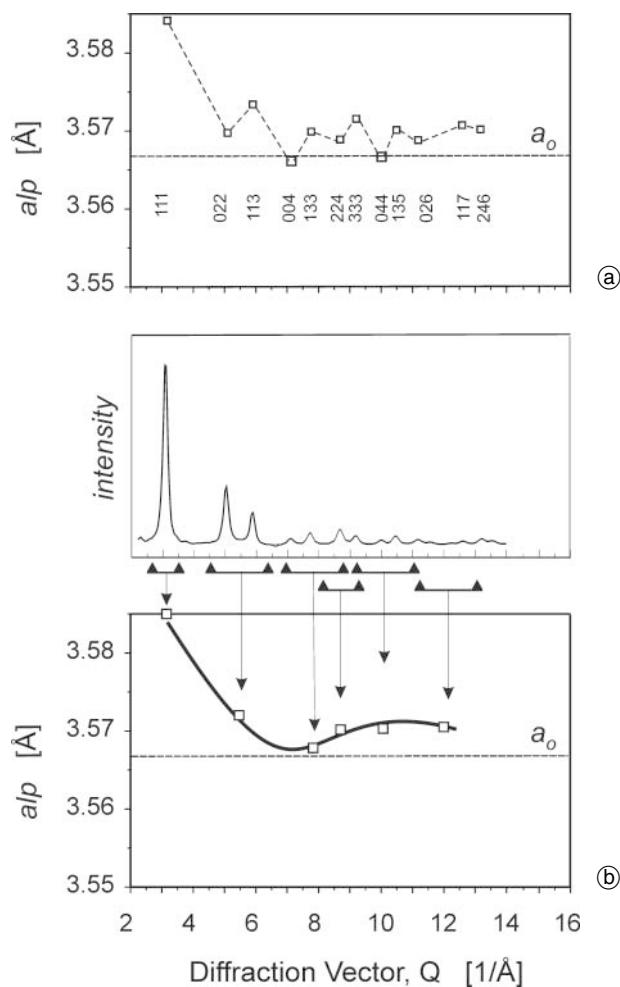


**Fig. 4.** Illustration of two methods of elaboration of theoretical powder diffraction data of a nanocrystalline powder, with a cube-like shape grains, using the  $alp$  methodology: (a),  $alp$  values calculated from d-values of individual  $hkl$  Bragg reflections; (b),  $alp$  values calculated for groups of reflections for selected  $Q$ -ranges (the  $alp$  values were “refined”, for a given  $Q$ -range, with the Rietveld program DBWS-9807).

visualization convention is used in other graphs of this paper.  $Alp$ - $Q$  plots obtained for grouped reflections for cubic grains of different size are shown in Fig. 5. As seen from this figure, the differences between the calculated  $alp$  values and the lattice parameter of the model decrease with an increase in the grain size.

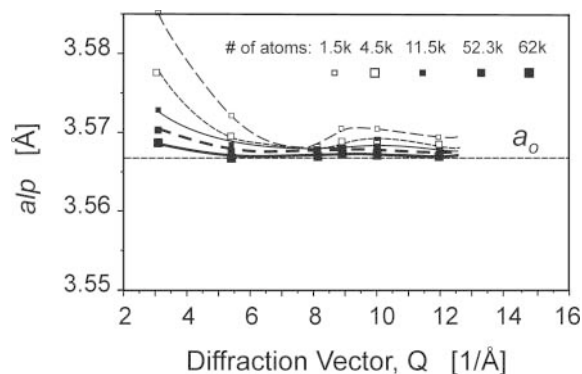


**Fig. 5.**  $Alp$ - $Q$  plots with  $alp$ 's determined from the theoretical diffraction patterns for groups of Bragg reflections in several  $Q$ -ranges, calculated for diamond grains with a perfect crystal lattice for different grain sizes.

## 3.2 Nanocrystals with non-uniform structure

### 3.2.1 Origin of surface strain and internal pressure

The surface of a crystal is a region where the stress tensor differs from that in the bulk of the solid; the surface shell can be considered as a separate phase with its specific structural and physical properties. Equilibrium spacings between atoms are different for two- than for three-dimensional, relaxed lattices. Therefore, the two-dimensional layer of molecules on the surface of a crystal must be either extended or compressed if its intermolecular spacings are to match those of the underlying 3-D lattice.

Following the general concept of the surface tension, the surfaces of a single crystal are in a state of tension (its magnitude specific for each face) that subjects the interior of the crystal to stresses. As a result, the developed stresses may be expected to lead to an internal pressure that manifests itself by a compression of the crystal lattice [3, 26, 31, 32, 34]. This effect can, in principle, be measured experimentally as a change of the lattice parameters of the interior of the crystallite (the grain core). As shown in Section 3.1, for very small crystals determination of the lattice parameters is not a trivial problem. The problem becomes even more complex when internal strains and stresses exist in the surface shell of the grains. In a diffraction experiment it is practically impossible to separate the signals from the grain core and those from the surface shell: the beam scattered by the core atoms interferes with that scattered by the surface atoms. As we will show in this work, an appropriate analysis of powder diffraction data allows gaining an insight into the real structure of nanocrystalline powders.

### 3.2.2 Effect of surface strain on $alp$ values of nanocrystals

We applied the  $alp$  concept of the analysis of powder diffractograms described above for nanocrystals with a perfect crystal lattice, to a core-shell model of small crystals. We assumed that a nanocrystal is composed of a core and of the surface shell that has a slightly different structure. In this work we used the model of a spherically shaped nanocrystal where the grain core has a uniform crystallographic structure and is unambiguously characterized by the lattice parameter  $a_0$  (we used  $a_0 = 3.5667$  of the relaxed diamond lattice). We assumed that the atomic structure of the surface layer is strongly correlated with the parent structure of the grain: it is basically the structure of the core but centro-symmetrically deformed, as shown schematically (for compressed surface layer) in Fig. 6. To simplify the description of the model, we introduced the parameter  $a_s$  which corresponds to the lattice parameter  $a$  at the outmost atomic layer of the particle (Fig. 6). Assuming that the arrangement of atoms in the surface shell is similar to that in the grain core, the value of  $a_s$  is a fraction of the lattice parameter  $a_0$ . Without compression the width of the surface layer would be  $s_0$ . The actual values of the interatomic distances within the surface shell can be expressed as a function of the distance from the particle center and vary between  $a_0$  in the grain core (at distances

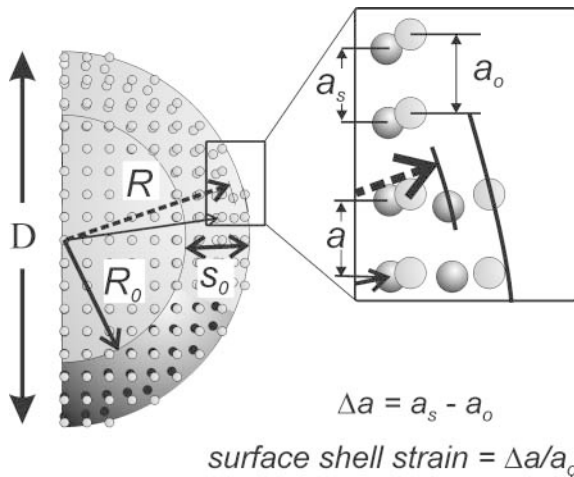


**Fig. 6.** Tentative model of a nanocrystal with strained (here: compressed) surface layer.  $S_0$ , thickness of the surface shell without compression;  $a_0$ , lattice parameter of the grain core (relaxed lattice);  $a_s$ , lattice parameter at the outmost atomic plane of the (strained) surface.

$r = R_0$ ) and  $a_s = a_0 + \Delta a$  (for  $r = R$ ). The ratio  $\Delta a/a_0$  is quantifying the surface strain. (Note: in a complete physical model of a crystallite the real shape and different properties of the atomic planes confining the crystal should be accounted for. The properties of diamond surfaces were discussed by Lurie and Wilson [49].)

It was found that, for our simple model of the crystal grain, the effect of the dependence of strains in the surface layer on radius could be ignored. Therefore, to simplify the modeling, the  $alp$  values were calculated assuming uniform compression of the surface shell lattice. The  $alp$ - $Q$  plots discussed below were calculated for 5 nm diameter diamond crystallites with the surface shells 0.5 and 0.7 nm in thickness and all interatomic distances within the shell compressed by 3 (5)%. (For a spherical crystallite of 5 nm in diameter, the surface shell 0.5 and 0.7 nm thick contains about 50% and 60%, respectively, of all atoms in the grain.) The  $alp$  values were calculated by refinement of the  $alp$  values for selected  $Q$ -ranges (c.f. Fig. 4). The results of the calculations are shown in Fig. 7. Figure 7a shows that, for the surface layer compressed by 3%, the decrease of the calculated  $alp$  values in the whole  $Q$ -range relative to that of a relaxed lattice is approximately  $-0.3\%$ , i.e. 10 times less than the strain implemented in the surface shell. Proportionally larger shift in the  $alp$  positions is observed for the model with the surface shell compressed by 5% (Fig. 7a). As expected, larger deviations are observed for the grain with a thicker surface shell (Fig. 7b). The general shape of  $alp$ - $Q$  plots for crystallites with a strain present in the surface shell is basically the same as that calculated for similar crystallites with a relaxed crystal lattice (Figs. 5 and 7). (Note: a presence of strain in the surface shell leads to some asymmetry of the Bragg lines and, subsequently, to a larger error in determination of the specific  $alp$  values; we estimate that the error increases by  $0.001\text{\AA}$  relative to that for a perfect lattice, c.f. Section 3.1 and Figs. 2–5.) The  $alp$ - $Q$  plots calculated for our simple core-shell model analyzed in this work were used for an estimation of the magnitude of strains present in the surface shell of diamond nanocrystals studied experimentally (c.f. Section 3.3.2). Note

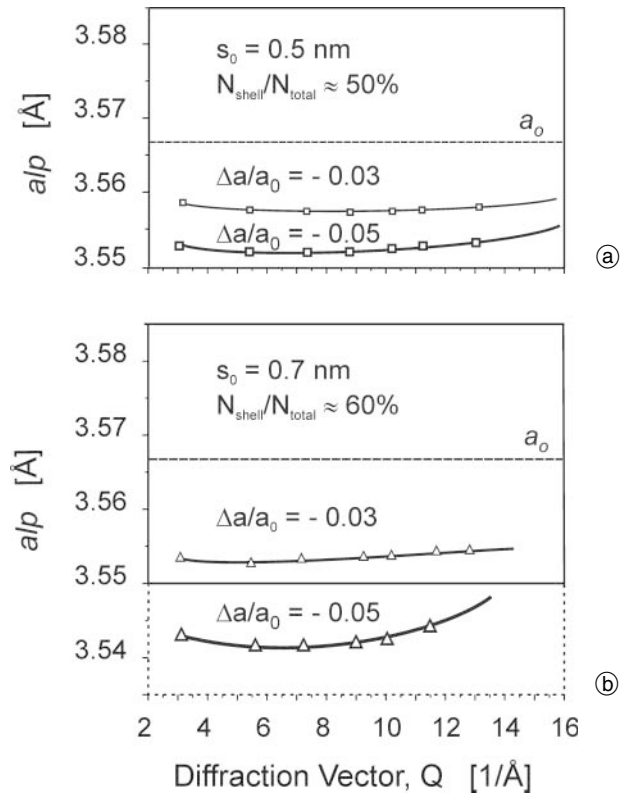


**Fig. 7.**  $alp$ - $Q$  plots calculated for models of  $d = 5$  nm diameter diamond nanocrystals for different degrees of compression of the shell lattice relative to that of the core. (a),  $s_0 = 0.5$  nm; (b),  $s_0 = 0.7$  nm.

that a presence of internal strains alone would lead to a change of all  $alp$  values by the same amount without changing the shape of the dependence of  $alp$  on  $Q$ .

### 3.3 Experimental

#### 3.3.1 Experimental procedures

We examined four diamond polycrystalline powders, each having a different average grain diameter. The powders A and B were synthesized from graphite using the high shock blow method: powder A is “ultradiamond 90” supplied by Ultradiamond Technologies Inc. (373 Highland Avenue, Suite 201, Somerville, MA 02144, USA, www.ultradiamondtech.com), powder B was supplied by Nanodiamond and Nanotechnologies ALITEX (ul. Vernadskogo 35, Kiev, Ukraine, www.alitex.com.ua). Powder C was a commercial DP 1–2 Micron Polycrystalline Diamond Powder synthesized by an exclusive compaction process, manufactured by Mypodiamond Inc. and supplied by Microdiamant Rudolf Spring Inc. (Kreuzlinger Strasse, CH-8574 Lengwil, Switzerland, www.microdiamant.com). This powder is composed of nanocrystallites with the average diameter of 12 nm agglomerated into 1–2 micron particles.

We performed a number of powder diffraction experiments using synchrotron sources and collecting data in a large  $Q$ -range. We used Stations ID11 at ESRF and BW5 at HASYLAB (wavelength  $0.1$ – $0.2\text{\AA}$ ), and SNBL Station at ESRF (wavelength  $0.5$ – $0.7\text{\AA}$ ) approaching  $Q_{\max} = 10$ – $15\text{\AA}^{-1}$ . For each X-ray diffraction experiment the specific  $alp$  values were determined with reference to

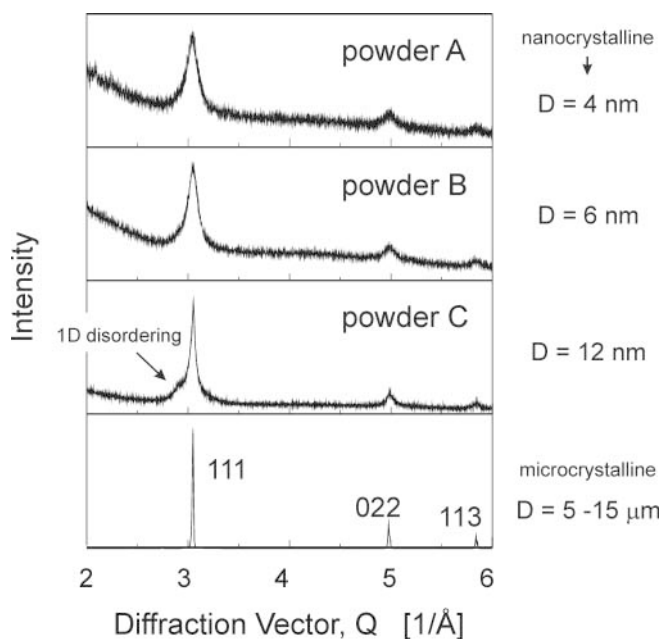


**Fig. 8.** Low- $Q$  part of X-ray diffraction patterns measured experimentally for four diamond polycrystalline samples with different grain diameters: 4 nm, 6 nm, 12 nm, and 5–15  $\mu\text{m}$ . The small peak of powder C is due to one-dimensional disordering.

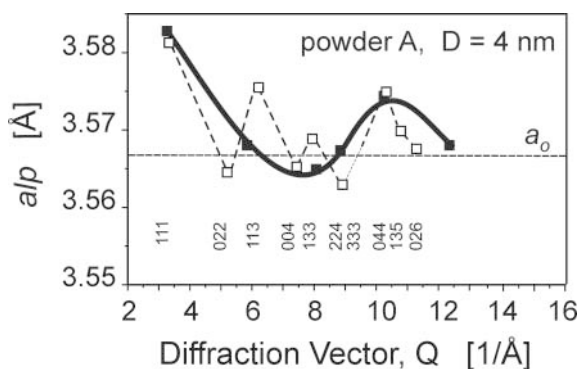
Si microcrystalline powder used as a standard and measured in the same experimental set-up before and after the sample scan.

Neutron diffraction measurements were done using the HIPD diffractometer at LANSCE in Los Alamos National Laboratory, in the diffraction vector range approaching  $Q_{\text{max}} = 26 \text{ \AA}^{-1}$ .

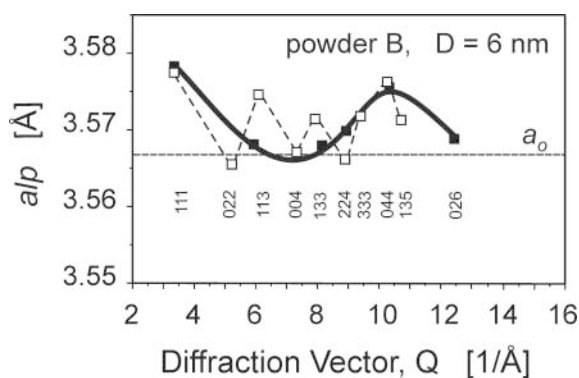
### 3.3.2 $Alp$ - $Q$ relations

Fig. 8 shows X-ray diffraction patterns of the samples. All samples show the cubic diamond structure except for powder C that exhibits a pronounced one-dimensional disordering and, as a result, shows a trigonal, non-cubic symmetry.

Figs. 9 and 10 present experimental  $alp$ - $Q$  plots of as-synthesized (and stored in air) samples (powders A and B, respectively), Figs. 11 and 12 show  $alp$ - $Q$  plots of 4 and



**Fig. 9.** Experimental  $alp$ - $Q$  results determined from X-ray (synchrotron) diffraction experiments with raw (untreated) powder A. Open squares and solid squares,  $alp$  values calculated from individual and groups of reflections, respectively.  $a_0$  is the lattice parameter of micro-size powder.



**Fig. 10.** Experimental  $alp$ - $Q$  results determined from X-ray (synchrotron) diffraction experiments with raw (untreated) powder B. Open squares and solid squares,  $alp$  values calculated from individual and groups of reflections, respectively.  $a_0$  is the lattice parameter of micro-size powder.

12 nm diamond powder samples after their annealing in vacuum at 400  $^{\circ}\text{C}$  for 4 hrs (powders A and C, respectively). The  $alp$  values were determined using the two methods presented in Fig. 4: calculation of  $alp$  for individual Bragg lines and for specific  $Q$ -ranges. All experimental  $alp$ - $Q$  plots show clear similarities to the theoretical  $alp$  values calculated for models of diamond nanocrystals shown in Figs. 3 and 5, both for individual and group  $alp$ - $Q$  results.

From Fig. 3 it follows that, in principle, from the magnitude and distribution of the  $alp$  values (calculated for individual reflections) the shape of the crystallites can be deduced. However, all our nanopowders show a distribution of grain sizes and have, most likely, non-uniform and various shapes. Accounting for such parameters of the materials would be a very complex and difficult task. For practical reasons we focused on the general, and most meaningful (at this moment) features of the experimental  $alp$ - $Q$  plots obtained by refining  $alp$  values for specific  $Q$  ranges.

The  $alp$ - $Q$  plots presented in Figs. 9 to 12 have shapes consistent with those calculated theoretically and shown in Fig. 5: the largest  $alp$  is at the smallest  $Q$  followed by a minimum occurring within the range  $6 \text{ \AA}^{-1} < Q < 8 \text{ \AA}^{-1}$  and the next maximum at about  $Q = 10 \text{ \AA}^{-1}$ . The span between the minimum and the second maximum is larger

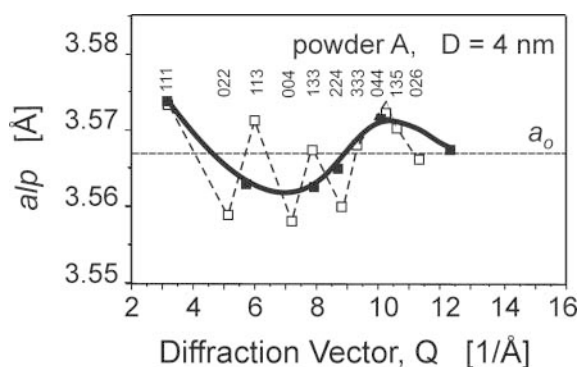


**Fig. 11.** Experimental  $alp$ - $Q$  results determined from X-ray (synchrotron) diffraction experiments with outgassed powder A. Open squares and solid squares,  $alp$  values calculated from individual and groups of reflections, respectively.  $a_0$  is the lattice parameter of micro-size powder.

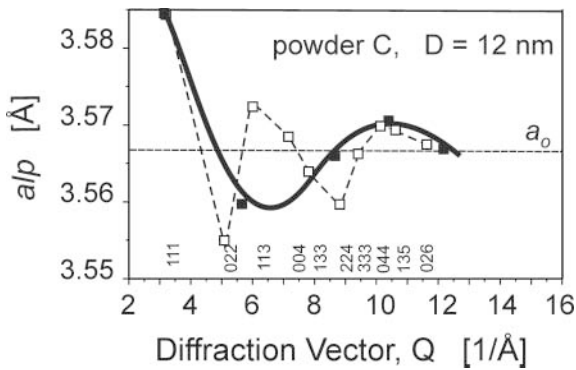


**Fig. 12.** Experimental  $alp$ - $Q$  results determined from X-ray (synchrotron) diffraction experiments with outgassed powder C. Open squares and solid squares,  $alp$  values calculated from individual and groups of reflections, respectively.  $a_0$  is the lattice parameter of micro-size powder.

for the experimental than theoretical results. This is probably due to non-uniform, specific shapes of the diamond crystallites, the subject that is not investigated in the present work. It should be noticed that the  $alp$ - $Q$  plots obtained for individual Bragg lines give a clear evidence that small diamond crystals of our samples are not spherical in shape.

We focused our attention on the position of the minimum of  $alp$ - $Q$  plots that varies from sample to sample. In the theoretical plots the first minimum in  $alp$  is close to the lattice parameter of a relaxed diamond lattice,  $a_0$  (Fig. 5). In Figs. 9 and 10 the minimum  $alp$  value is smaller than  $a_0$  by  $0.004 \text{ \AA}$  ( $-0.11\%$ ) and  $0.002 \text{ \AA}$  ( $-0.06\%$ ), for raw powders A and B, respectively. The question is, what is the origin and location of the apparent compressive strain in the grain that affects the  $alp$  value. If, following a general concept of surface tension, it is assumed that the grain surface is infinitely thin then the compression of the diamond lattice would be associated with a presence of an internal pressure in the particles [26] and/or with a presence of surface shell with the diamond lattice compressed relative to the interior of the crystallite (the core-shell model, Fig. 6, discussed in Section 3.2). Fig. 7 shows that a presence of compressed surface shell leads to a decrease of all  $alp$  values in the entire  $Q$ -range, but the decrease is greater at low than at large  $Q$  vectors; that means that the nature of the  $alp$ - $Q$  relation changes. Assuming that the core-shell model is appropriate for diamond nanocrystals, and that no internal pressure is present in the bulk (i.e. that the lattice parameters of the grain core are equal to that of the relaxed diamond lattice) we can evaluate the strain in the surface shell by comparing our experimental results to those shown in Fig. 7. Assuming the thickness of the surface shell at  $0.5 \text{ nm}$ , the estimated strain is  $-1\%$  (approximately  $1/3$  of the decrease in the  $alp$  values calculated for the  $3\%$  strain in the surface shell, Fig. 7a), and even lower assuming that the surface shell is thicker ( $0.7 \text{ nm}$ , Fig. 7b). (We discuss these results again in Section 4.2 in connection with the PDF analysis of our neutron diffraction data.)

Our estimates of the magnitude of strains in the lattice depend on the assumed thickness of the surface layer. The analysis of our modeling results showed, that the thickness

of the layer affects the shape of the  $alp$ - $Q$  curves; for greater strains the  $alp$  values approach the lattice parameter of the core at lower  $Q$  values [41]. Based on that, we estimated that the thickness of the surface layer in our samples is on the order of  $0.5$ – $0.7 \text{ nm}$ , and used these values for our calculations and discussions presented in this paper.

The minimum  $alp$  values for the vacuum annealed powders A and C (Figs. 11 and 12, respectively) are much smaller than those observed for raw (as-supplied, un-treated) powders (Figs. 9 and 10): the minimum  $alp$  is at  $0.006 \text{ \AA}$  ( $-0.18\%$ ) and  $0.008 \text{ \AA}$  ( $-0.25\%$ ) below  $a_0$ . Again, referring to the core-shell model and Fig. 7 we estimated the surface strains at  $-2\%$  and  $-3\%$  for samples A and C, respectively. A comparison of the  $alp$ - $Q$  plots of as-synthesized and vacuum-annealed powder A (Figs. 9 and 11, respectively) shows a strong decrease of the  $alp$  values after outgassing. The same procedure of outgassing applied to powder C did not lead to any changes in the  $alp$  values: the  $alp$ - $Q$  plots of vacuum cleaned and raw (not shown) samples are identical. The difference between the powders A and C is that in powder A the grains are basically loose and well separated, while in samples C they form relatively large, several micrometer in size agglomerates. As a result, the (effective) specific surface of powder C is 3 orders of magnitude smaller than that of powder A ( $1$ – $2$  vs.  $300 \text{ m}^2/\text{g}$ , respectively). The strong effect of outgassing of powder A on the experimentally determined  $alp$  values is a clear indication that the strain develops in the surface shell of the grains. Obviously the adsorption of foreign atoms at the surface leads to relaxation of the strains present in the surface shell and, in the case of diamond samples, to a decrease in the  $alp$  values.

Powder diffraction experiments performed using X-ray sources were duplicated using neutron scattering technique. Due to a very complex shape of individual Bragg reflections measured in TOF experiments with the HIPD diffractometer, determination of the positions of individual reflections is practically impossible. Therefore we calculated the  $alp$  values for specific  $Q$ -ranges only using the GSAS refinement program of Larson and Von Dreele [50] and its graphical interface by Toby [51]. The  $alp$ - $Q$  plots determined for the annealed powders A and C are shown in Fig. 13. A very close agreement between these results

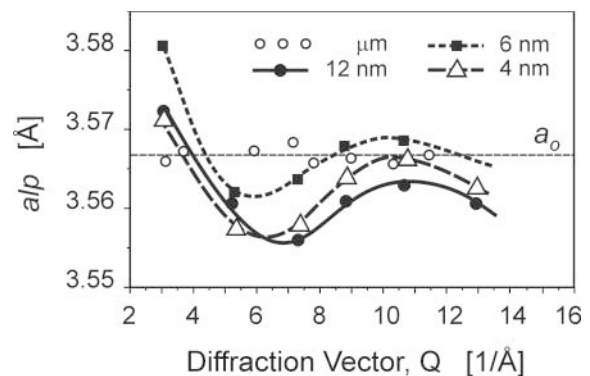


**Fig. 13.**  $alp$ - $Q$  results determined from neutron diffraction experiments (HIPD, LANSCE, Los Alamos) obtained with four outgassed diamond powders of different grain size. The  $alp$  values were calculated for groups of reflections.

and those obtained for X-ray sources (Figs. 9 to 12) exists. Some differences between the absolute  $alp$  values determined from X-ray and neutron data were observed. They are apparently due to differences in the instruments calibrations and/or the software used for the data elaboration. For our studies, which are focused on differences between samples of different grain size, those differences are insignificant.

#### 4. Atomic Pair Distribution Function approach: examination of short-range order in nano-crystals

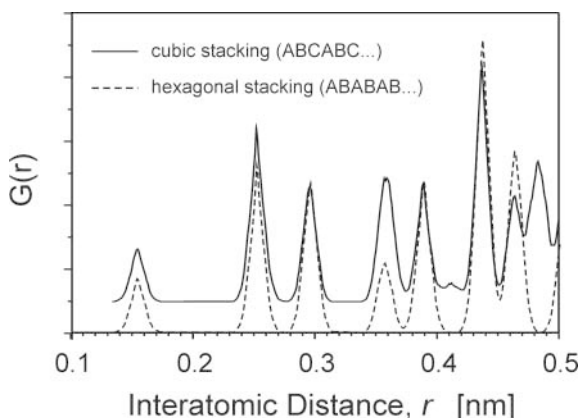
##### 4.1 Theoretical PDF results

We calculated theoretical  $G(r)$  functions for models of nanocrystals discussed in previous sections. In the calculations we accounted for thermal motions of the atoms by assuming the amplitude of isotropic, harmonic oscillations of 0.1 Å. The presence of thermal motion, implemented in the models as a positional static disorder of all atoms, leads to broadening of the lines on the  $G(r)$  plots and makes the theoretical plots more compatible with those obtained experimentally.

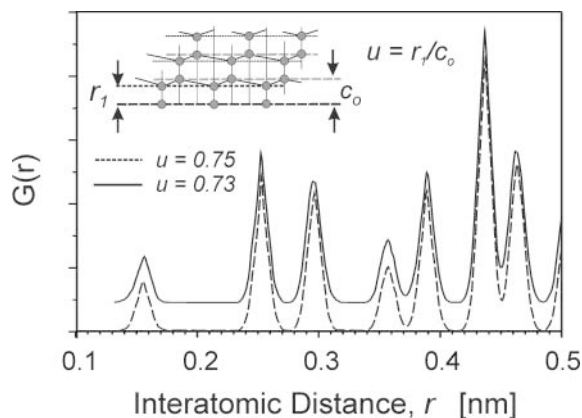
In this work we examined only the first seven shortest interatomic distances in the diamond lattice (these distances are shown schematically on the cross-sections through the cubic diamond lattice, c.f. Fig. 18a).

Fig. 14 shows  $G(r)$  functions calculated for models of a diamond crystal with cubic (ABC) and hexagonal (AB) type layer stackings. The only difference between the  $G(r)$ 's of the cubic and hexagonal structures are different populations (peak intensities) for distances corresponding to  $r_4$  and  $r_7$  spacings, and an appearance of one more maximum just beyond  $r_7$  (Fig. 14). The  $G(r)$  function presented in Fig. 14 was calculated for a perfect diamond lattice with lattice parameter  $a_0 = 3.5667$  Å. (Note that a hydrostatic (i.e. isotropic) compression of diamond would lead to a proportional decrease of all interatomic distances.)

In close-packed structures built of hexagonal layers, a change of the lattice symmetry from cubic to trigonal is usually accompanied by a change in some inter-atomic



**Fig. 14.** Theoretical Atomic Pair Distribution Function,  $G(r)$ , of a perfect diamond lattice with cubic (solid line) and hexagonal (dashed line) layer stackings.



**Fig. 15.** Theoretical Atomic Pair Distribution Function,  $G(r)$ , of a diamond lattice with cubic layer stacking and different  $u$  parameters.

distances in the lattice. The spacing that is sensitive to such change is the distance between two hexagonal layers lying in the lattice one above another and stacked along trigonal axis  $c$ ; this distance corresponds to  $r_1$  in  $G(r)$  plots (Fig. 15). This change in the structure is quantified by the parameter  $u$ . Fig. 15 shows theoretical  $G(r)$  functions calculated for cubic layer stackings with the parameter  $u = 0.75$  (which corresponds to the perfect cubic lattice) and a structure with somewhat different  $u$  value (assumed as 0.73) consistent with trigonal lattice symmetry. The important result of this calculation is, that a decrease in the  $u$  value leads to a change in only three out of the seven analyzed distances:  $r_3$ ,  $r_6$ , and  $r_7$  shift towards smaller values, while other spacings remain unchanged.

Fig. 16 presents theoretical  $G(r)$  functions computed for models of spherical 5 nm diameter diamond crystals

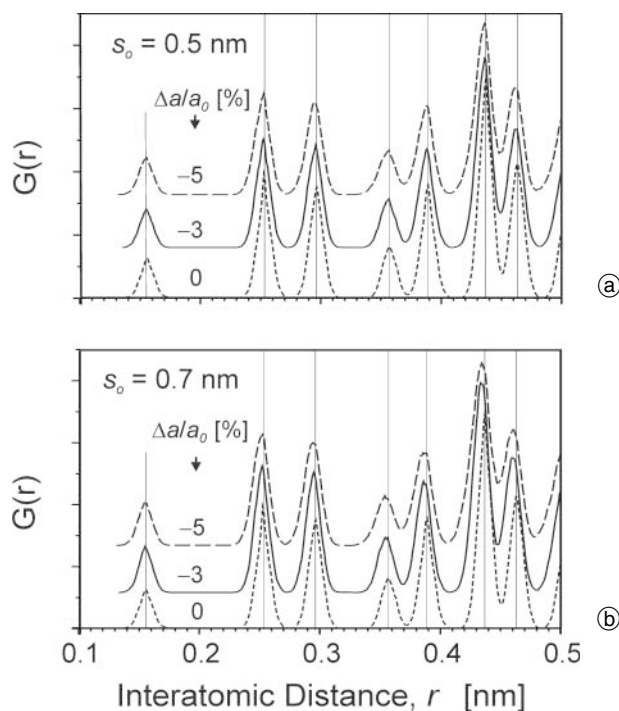


**Fig. 16.** Atomic Pair Distribution Functions,  $G(r)$ , calculated for models of spherical (5 nm in diameter) diamond nanocrystals with different degree of compression of the surface shell lattice relative to that in the core. (a),  $s_0 = 0.5$  nm; (b),  $s_0 = 0.7$  nm.

with strained surface shell; the same models were used to calculate the  $alp$ - $Q$  data shown in Fig. 7. A presence of strains in the surface shell leads to shifts of individual peaks on the  $G(r)$  plot, a different shift for each atomic pair. For the surface shell 0.5 nm thick, the positions of the peaks  $r_1$  and  $r_4$  remain unchanged while, for a given strain in the surface, other peaks decrease by a similar value.

## 4.2 Experimental results

We have done the PDF analysis of powder diffraction results of diamond samples with the same raw data used to obtain the  $alp$ - $Q$  plots shown in Fig. 13. The diffraction data were collected in the  $Q$ -range up to  $30 \text{ \AA}^{-1}$  and above. Due to a very large broadening and increasing overlap of the Bragg lines with an increase in  $Q$ , we were able to obtain  $alp$ - $Q$  plots only up to  $Q = 15 \text{ \AA}^{-1}$ . The useful part of the patterns used for PDF analysis extended to  $Q = 26 \text{ \AA}^{-1}$ . PDF analysis was made using PDFgetN program of Peterson et al. [52].

Fig. 17 presents the experimental  $G(r)$  functions determined for our four diamond powders. To resolve the positions of individual peaks we fitted (refined) the peak shapes using the Gaussian function taking the positions of the peak maxima. The character of the  $G(r)$  function of powder C shows some differences relative to the others: an apparent increase in  $G(r)$  around 0.48 nm (marked by an asterisk) and a change in the relative intensity of peaks at  $r_4$  and  $r_5$ . As shown above in Fig. 14, this behavior of  $G(r)$  may be associated with a presence of hexagonal-type stackings in the diamond lattice. This observation coincides with a presence of diffuse scattering preceding the (111) diamond reflection that indicates a presence of one-dimensional disordering in the sample (Fig. 8).

The results of elaboration of the experimental  $G(r)$  functions, interatomic distances  $r_1$ – $r_7$  for different (aver-

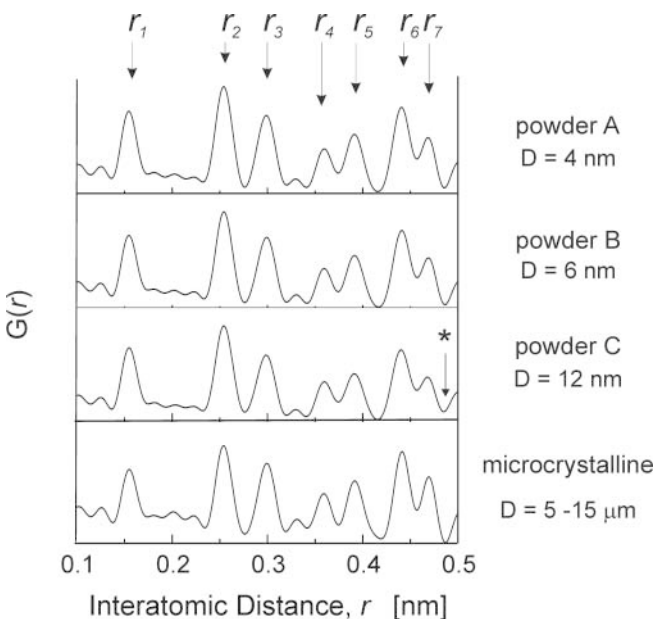


**Fig. 17.** Experimentally determined  $G(r)$  functions of four polycrystalline diamond powders of different grain diameters: 4 nm, 6 nm, 12 nm, and 5–15  $\mu\text{m}$ . Notice an increase in  $G(r)$  at 4.85  $\text{\AA}$  and a change of relative intensities of the maxima at  $r_4$  and  $r_5$  in sample C.

age) grain sizes of the samples, are shown in Fig. 18b. The interatomic distances obtained from our measurements of microcrystalline diamond differ from the well established literature data, i.e. the experimental value of  $r_4$  (3.5918  $\text{\AA}$ ), which corresponds to the cubic lattice parameter  $a_0$ , is slightly different than the literature data of 3.5668  $\text{\AA}$ . The discrepancy is apparently the result of not fully accurate calibration of the instrumental parameters used by the computer program for data reduction and calculation of  $G(r)$ . The most important features of the experimental  $G(r)$  functions of nanocrystalline diamonds are as follows:

- (1) The shifts of  $r$ -distances are diversified; they are not proportional to the  $r$ -values, and are even of different directions (sign). This is a clear indication that the shifts are not the result of a hydrostatic-type compression of the diamond lattice, and suggests that the structure of the material is heterogeneous. The relative change of individual  $r$ -values of the powder with the smallest grains (A) is between  $-0.3\%$  and  $+0.08\%$ . These values are similar to those obtained from  $alp$  method: the minimum  $alp$  value measured for this sample is 0.2% below the lattice parameter  $a_0$  of the relaxed diamond lattice (Fig. 13).
- (2) The changes of  $r$ -values for powders A and B, relative to the microcrystalline sample, show similar tendencies. However, for powder A (smaller grains) these changes are always larger than those measured for powder B (larger grains). This suggests that the origin of these shifts is similar and consistent with the core-shell model. Those changes can be explained assuming that the surface shell in both samples has similar thickness and similar lattice strain irrespective of the crystallite size. The relative number of surface-to-core atoms increases with a decrease of the grain size (approximately 50 and 30% of the total number of atoms in 4 and 6 nm diameter grains, respectively) what is consistent with larger shifts of (averaged)  $r$ -values in powder A than B.
- (3) Powder C behaves quite differently than A and B (in Fig. 18 the  $r$ -values of sample C are placed in circles). The largest differences between the  $r$ -values determined for powders A and B and for powder C are observed for distances  $r_3$ ,  $r_6$ , and  $r_7$ . This can be explained by deformation of the diamond lattice associated with one-dimensional disordering and a trigonal not cubic symmetry of the lattice in strongly agglomerated powder C. The reason for strong shifts of only three  $r$  values is explained in Fig. 15 which shows, that a change of the parameter  $u$  from 0.75 to 0.73 leads to shortening of only these three interatomic distances. This small effect, clearly visible in the  $G(r)$  plot, is practically impossible to detect with the Bragg-type analysis of nanocrystalline materials (due to very broad diffraction lines).
- (4) For powders A and B, the distances  $r_1$ ,  $r_2$ , and  $r_4$  change much less with a change in the grain size than  $r_3$ ,  $r_6$  and  $r_7$ . It is highly unlikely that the cu-

bic lattice of diamond could be compressed anisotropically. Therefore, a reasonable explanation of the diverse changes of different  $r$ -distances is, that these differences are associated with an anisotropic nature of the strains present at the surfaces terminating the nanocrystals. The very simple model applied in the current work, which assumes spherical grain shape and radial symmetry of the surface

strain, is insufficient for a more detailed interpretation of our experimental results at this moment.

- (5) Of the seven  $r$  distances  $r_4$  behaves differently than the others. This distance corresponds to the edge of the cubic unit cell of diamond and increases with a decrease in the grain size. This is an important sign that a reference to only one lattice distance, like  $r_4$  which can be identified with the lattice parameter

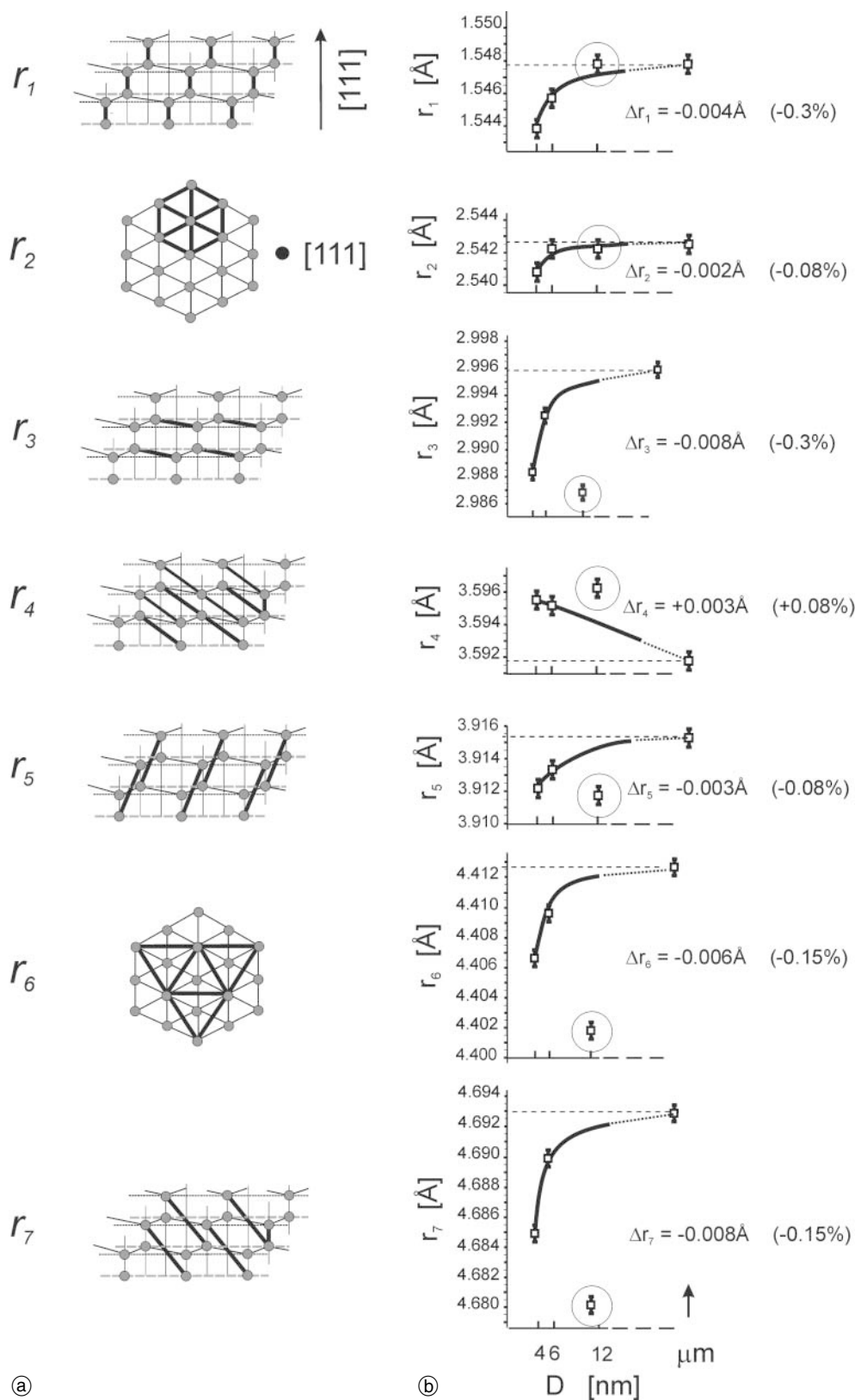


**Fig. 18.** Interatomic distances determined from experimentally obtained  $G(r)$  functions of different polycrystalline diamond powders. (a), schematic presentation of interatomic distances  $r$ ; (b), experimentally determined inter-atomic distances in the powders.

(a)

(b)

$a_0$  of the diamond structure, may easily lead to non-unique or even erroneous conclusions: as shown above, while most of the interatomic distances become shorter (compressed), the lattice parameter seems to get larger.

Differences between shifts of interatomic distances show very clearly that changes in the distances in small size crystallites do not relate in a simple, straightforward manner to hydrostatic compression of the diamond lattice which, according to the general theory of surface tension, should lead to a presence of internal pressure in the crystallite interior and to a hydrostatic-like compression of the diamond lattice. However, all the above observations do not mean that an internal pressure is not present in small diamond crystals. On the contrary, it may be expected that, consistent with the concept of the surface tension, a generation of strains in the surface layer is associated with generation of an internal pressure in the grain interior. The observed increase of the (average) distance  $r_4$  in diamond nanocrystallites suggests, that in response to compression of the surface shell the cores of the diamond crystallites expand in size.

## 5. Summary and conclusions

The methodology of the structural analysis of micrometer-size polycrystals is well established and approximations made for description of the structure of such materials and for the analysis of their diffraction data provide satisfactory results. However, the conventional tools developed for elaboration of powder diffraction data are not directly applicable to nanocrystals:

- (i) Conventional powder diffraction techniques and appropriate methods of their elaboration have been developed for materials showing a perfect, three-dimensional, periodic order in an infinite crystal lattice. In nanocrystals, due to their small size, the structural and other properties of the surface atoms are different and can dominate over the effects determined by the bulk atoms. This effect is clearly observed in our diffraction experiments.
- (ii) Nanoparticles have a complex structure that resembles rather a two-phase than a uniform, one-phase material. Therefore the definitions and parameters used for characterization of the atomic structure of simple, crystallographically uniform phases are insufficient for a description of the complex structure of nanocrystals;

This work shows limitations of a conventional structural analysis approach, and demonstrates an application of a new method of evaluation of diffraction data of nano-size polycrystalline materials. The applicability and usefulness of the method has been tested using our experimental powder diffraction data of several different diamond powder samples. We have demonstrated a qualitative agreement between the experimental results and those obtained by numerical modeling using our *alp* concept methodology. The *alp* analysis of the experimental results, combined with the PDF method, provides a strong support to the concept of a two-phase structure of nanocrystalline

grains. The model of a spherical crystallite with radial symmetry of strain in the surface shell is a very rough approximation of strains present in real crystals. A more complete evaluation of powder diffraction data of specific nanocrystalline materials requires a wider spectrum of structural models. In an advanced physical model of real materials one should account for anisotropic strain field in the planes terminating real crystallites as well as for the shape and size distribution of nanocrystals in the samples. The work on these issues is in progress.

*Acknowledgments.* This work was supported by the Polish Committee for Scientific Research – grant PBZ/KBN-013/T08/30, the Polish-German Project POL-00/009 and in part by the EC Grant “Support for Centers of Excellence” No. ICA1-CT-2000–70005, DESY – HASYLAB Project II-99–053, ESRF Project HS-1463. Experimental assistance from the staff of the Swiss-Norwegian Beam Lines at ESRF is gratefully acknowledged. Support of the Office of Biological and Physical Research of NASA and of the US Department of Energy/LANSCE is greatly appreciated.

## References

- [1] Edelstein, A. S.; Cammarata, R. C. (Eds.): *Nanomaterials: Synthesis, Properties and Applications*, Institute of Physics Publishing, Bristol and Philadelphia 1996.
- [2] Fujita, F. E.: *Physics of New Materials*. Springer Series in Materials Science 1998.
- [3] Howe, M. J.: *Interfaces in Materials*. John Wiley and Sons, Inc. 1997.
- [4] Suryanarayana, C.: *Non-equilibrium Processing of Materials*, Pergamon 1999.
- [5] Wang, Z. L.: *Characterization of Nanophase Materials*, Wiley-VCH 2000.
- [6] Banfield, J. F.; Navrotsky, A. (eds.): *Nanoparticles and the Environment* (eds.). *Reviews in Mineralogy and Geochemistry* **44**. Mineralogical Society of America 2001.
- [7] Averback, R. S.: Sintering and Deformation of Nano-grained Materials. *Z. Phys.* **D26** (1993) 84–88.
- [8] Buffat, Ph.; Borel, J. P.: Size effect on the melting temperature of gold particles. *Phys. Rev.* **A13** (1976) 2287–2298.
- [9] Inoue, A.; Hishimoto, K.: *Amorphous and Nanocrystalline Materials: Preparation, Properties and Applications*. Springer 2001.
- [10] Qadri, S. B.; Yang, J.; Ratna, J. B.; Skelton, E. F.; Hu, J. Z.: Pressure induced structural transition in nanometer size particles of PbS. *Appl. Phys. Lett.* **69** (1996) 2205–2207.
- [11] Silvestri, M. R.; Schroeder, J.: The size dependence of the high-pressure phase stability of II–VI semiconductor nanocrystals. *J. Phys.: Condens. Matter* **7** (1995) 8519–8527.
- [12] Tolbert, S. H.; Alivisatos, A. P.: Size dependence of the solid-solid phase transition in CdSe nanocrystals. *J. Phys.* **26** (1993) 56–58.
- [13] Wolf, D.; Merkle, K. L.: Correlation between the structure and energy of grain boundaries in metals. In: *Materials Interfaces: Atomic Level Structure and Properties* (Eds. D. Wolf and S. Yip), p. 87–150. Chapman and Hall, London 1992.
- [14] Lue, J. T.: A review of characterization and physical property studies of metallic nanoparticles. *J. Phys. Chem. Solids* **62** (2001) 1599–1612.
- [15] Choi, C. J.; Dong, X. L.; Kim, B. K.: Characterization of Fe and Co nanoparticles synthesized by chemical vapor condensation. *Scripta Mater.* **44** (2001) 2225–2229.
- [16] Harada, J.; Ohshima, K.: X-ray diffraction study of fine gold particles prepared by gas evaporation technique. *Surf. Sci.* **106** (1981) 51–57.
- [17] Solliard, C.; Flueli, M.: Surface stresses and size effect on the lattice parameter in small particles of gold and platinum. *Surf. Sci.* **156** (1985) 487–494.
- [18] Woltersdorf, J.; Nepijko, A. S.; Pippel, E.: Dependence of lattice parameters of small particles on the size of the nuclei. *Surf. Sci.* **106** (1981) 64–69.

- [19] Montano, P. A.; Shenoy, G. K.; Alp, E. E.; Schulze, W.; Urban, J.: Structure of Copper Microclusters Isolated in Solid Argon. *Phys. Rev. Lett.* **56** (1986) 2076–2079.
- [20] Tolbert, S. H.; Alivisatos, A. P.: The wurtzite to rock salt structural transformation in CdSe nanocrystals under high pressure. *J. Chem. Phys.* **102** (1995) 4642–4656.
- [21] Lan, Y. C.; Chen, X. L.; Xu, Y. P.; Cao, Y. G.; Huang, F.: Synthesis and structure of nanocrystalline gallium nitride obtained from ammonothermal method using lithium metal as mineralizator. *Mat. Res. Bulletin* **35** (2000) 2325–2330.
- [22] Boswell, F. W. C.: Precise Determination of Lattice Constants by Electron Diffraction and Variations in the Lattice Constants of Very Small Crystallites. *Proceedings of the Physical Society (London)* **A64** (1951) 465–476.
- [23] Zhao, Y. H.; Zhang, K.; Lu, K.: Structure characteristics of nanocrystalline element selenium with different grain sizes. *Phys. Rev.* **B56** (1997) 14322–14329.
- [24] Beck, Ch.; Ehses, K. H.; Hempelmann, R.; Bruch, Ch.: Gradients in structure and dynamics of  $Y_2O$  nanoparticles as revealed by X-ray and Raman scattering. *Scripta Mater.* **44** (2001) 2127–2131.
- [25] Brown, R. C.: The fundamental concepts concerning surface tension and capillarity. *Proc. Royal Soc.* **59** (1947) 429–448.
- [26] Defay, R. and Prigogine, I.: Surface tension and adsorption. Longmans 1966.
- [27] Cammarata, R. C.: Thermodynamic model for surface reconstruction based on surface stress effects. *Surf. Sci. Lett.* **273** (1992) L399 – L402.
- [28] Cammarata, R. C.: Surface and interface stress effects on interfacial and nanostructured materials. *Mater. Sci. Eng.* **A237** (1997) 180–184.
- [29] Gilman, J. J.: Direct Measurements of the Surface Energies of Crystals. *J. Appl. Phys.* **31** (1960) 2208–2218.
- [30] Mays, C. W.; Vermaak, J. S.; Kuhlmann-Wilsdorf, D.: On surface stress and surface tension, II. Determination of the surface stress of gold. *Surf. Sci.* **12** (1968) 134–140.
- [31] Shuttleworth, R.: The Surface Tension of Solids. *Proceedings of the Physical Society (London)* **A63** (1950) 444–457.
- [32] Stoneham, A. M.: Measurement of surface tension by lattice parameter changes: theory for faceted microcrystals. *Journal of Physics C: Solid State Phys.* **10** (1977) 1175–1179.
- [33] Vermaak, J. S.; Mays, C. W.; Kuhlmann-Wilsdorf, D.: On surface stress and surface tension. I. Theoretical considerations. *Surf. Sci.* **12** (1968) 128–133.
- [34] Borel, J.-P.; Chatelain, A.: Surface stress and surface tension: Equilibrium and pressure in small particles. *Surf. Sci.* **156** (1985) 572–579.
- [35] Lennard-Jones, J. E.; Dent, B. M.: The change in Lattice Spacing at a crystal boundary. *Proc. Royal. Soc.* **A121** (1928) 247–259.
- [36] Molière, K.; Rathje, W.; Stranski, I. N.: Surface structure of ionic crystals. *Discuss. Faraday Soc.* **5** (1949) 21–32.
- [37] Alder, B. J.; Vaisnys, J. R.; Jura, G.: Penetration depth of surface effects in molecular crystals. *J. Phys. Chem. Solids* **11** (1959) 182–189.
- [38] Sanders, P. G.; Withey, A. B.; Weertman, J. R.; Valiev, R. Z.; Siegel, R. W.: Residual stress, strain and faults in nanocrystalline palladium and copper. *Mater. Sci. Eng.* **A204** (1995) 7–11.
- [39] Bish, D. L.; Post, J. E.: Modern Powder Diffraction. In: *Reviews in Mineralogy* **20**. Mineralogical Society of America, Washington DC 1989.
- [40] Young, R. A.: The Rietveld Method, International Union of Crystallography, Oxford University Press 1993.
- [41] Palosz, B.; Grzanka, E.; Gierlotka, S.; Stel'makh, S.; Pielaszek, R.; Lojkowski, W.; Bismayer, U.; Neuefeind, J.; Weber, H.-P.; Palosz, W.: Application of X-ray powder diffraction to nano-materials; determination of the atomic structure of nanocrystals with relaxed and strained surfaces. *Phase Transitions* (2002). In press.
- [42] Kaszkur, Z.: Powder diffraction beyond the Bragg law: study of palladium nanocrystals. *J. Appl. Cryst.* **33** (2000) 1262–1270.
- [43] Klug, H. P.; Alexander, L. E.: X-Ray Diffraction Procedures. John Wiley & Sons 1954.
- [44] Billinge, S. J. L.; Thorpe, M. F.: Local Structure from Diffraction. Plenum Press, New York and London 1998.
- [45] Loeffler, L.; Weissmueller, J.: Grain-boundary atomic structure in nanocrystalline palladium from X-ray atomic distribution functions. *Phys. Rev.* **B52** (1995) 7076–7093.
- [46] Zhu, X.; Birringer, R.; Herr, U.; Gleiter, H.: X-ray diffraction studies of the structure of nanometer-sized crystalline materials. *Phys. Rev. B.* **35** (1987) 9085–9090.
- [47] Bondars, B.; Gierlotka, S.; Palosz, B.: Program for simulation of diffraction patterns of small particles. *Mater. Sci. Forum* **133–136** (1993) 301–306.
- [48] Pielaszek, R.; Gierlotka, S.; Stel'makh, S.; Grzanka, E.; Palosz, B.: X-Ray Characterization of Nanostructured Materials. *Diffusion and Defect Forum* **208–209** (2002) 267–282.
- [49] Lurie, P. G.; Wilson, J. M.: The diamond surface: I. The structure of the clean surface and the interaction with gases and metals. *Surf. Sci.* **65** (1977) 453–475.
- [50] A. C. Larson, A. C.; Von Dreele, R. B.: General Structure Analysis System (GSAS). Los Alamos National Laboratory Report LAUR (2000) 86–748.
- [51] Toby, B. H.: EXPGUI, a graphical user interface for GSAS. *J. Appl. Cryst.* **34** (2001) 210–213.
- [52] Peterson, P.; Gutmann, M.; Proffen, Th.; Billinge, S. J. L.: PDFgetN, a user-friendly program to extract the total scattering structure function and pair-distribution function from neutron powder diffraction data. *J. Appl. Cryst.* **33** (2000) 1192.